Cross-Layer Performance Analysis for CSMA/CA Protocols: Impact of Imperfect Sensing

Jo Woon Chong, Dan Keun Sung, *Senior Member, IEEE*, and Youngchul Sung, *Senior Member, IEEE*

***Abstract*—In this paper, the performance of carrier-sense multiple access (CSMA)/collision-avoidance (CA) protocols in the presence of carrier-sensing errors is analyzed. Two types of carrier-sensing errors, i.e., false alarm and miss-detection, are considered, and their impact on the system performance is analyzed using a new CSMA/CA model based on a Markov chain capturing the sensing error at the physical layer. The system throughput and delay as functions of the sensing error probabilities, as well as other CSMA/CA parameters, are obtained, and their sensitivity with respect to a key physical-layer parameter, i.e., the sensing threshold, is analyzed for commonly used energy detectors or matched filters. It is shown that the throughput and delay sensitivity heavily depends on the ratio of the contention window size W to the frame length L, and the throughput is sensitive to the design of the sensing threshold when the ratio W/L is either small or large. The result provides guidelines about how to operate CSMA/CA considering imperfect sensing at the physical layer.**

***Index Terms*—Carrier-sense multiple access (CSMA)/collision avoidance (CA), carrier-sensing errors, delay, energy detector, matched filter, performance analysis, sensitivity, throughput, wireless local area networks (WLANs).**

I. Introduction

CARRIER-SENSE multiple access (CSMA)/collision avoidance (CA) is a well-established random-access protocol that has widely been used [1], [2]. In CSMA/CA systems, each user senses the channel to determine if the channel is available and accesses the channel depending on the sensing outcome. Recently, CSMA/CA has gained renewed attention since it was adopted in many wireless standards such as the wireless local area network (WLAN) and ZigBee [3], [4]. Several authors conducted an accurate performance analysis of the WLAN CSMA/CA to more efficiently operate the protocol [5]–[8]. The performance of the ZigBee CSMA/CA protocol was also evaluated by several authors [9]–[12]. In these analyses, however, carrier sensing errors were not considered, and thus, the physical-layer property was not properly captured. Recently, Krishnamurthy *et al.* [13] have measured the aggregated throughput of CSMA/CA systems by varying the carrier sensing threshold, which determines the sensing error probabilities, in an experiment and found that the aggregated throughput drastically changed with respect to the carrier sensing threshold value. Fuemmeler *et al.* [14] also conducted a similar study of the relation between CSMA and the carrier sensing threshold through simulation. This result shows that it is necessary to analyze the protocol under the sensing errors and to design the overall system by jointly optimizing the physical-layer characteristics and the medium access control (MAC)-layer parameters to improve the overall system performance. In our previous work, we analyzed the performance of the CSMA/CA protocol in the presence of carrier-sensing errors under the condition that the number of users is two [15]. Moreover, in [16], we extended the result to the n-user case $(n > 2)$ and analyzed the throughput and delay performance with sensitivity when the energy detector is adopted as a carrier sensor.

In this paper, we analyze the performance of the CSMA/CA protocol in the presence of carrier-sensing errors and examine the impact of the carrier sensing errors at the physical layer on the throughput and delay. With imperfect carrier sensing, the false-alarm error has an effect of extending the contention window (CW) size, and the miss-detection error results in two additional effects: shrinking the CW size and causing new additional collisions, compared with the perfect carrier-sensing CSMA/CA system. Furthermore, we consider commonly used carrier-sensing methods, i.e., energy detectors and matched filters, and investigate the sensitivity of throughput and delay with respect to the sensing threshold. It is shown that the sensitivity of the throughput and delay mainly depends on the ratio of the CW size W to the frame size L. The units of L and W are CSMA/CA backoff unit slots. It is also seen that the false-alarm probability p_f is the dominant factor for a large W/L, whereas the miss-detection probability p_m is the dominant factor for a small W/L. The loss by a poorly chosen sensing threshold is tolerable at intermediate values of the ratio W/L, whereas care should be taken in choosing the sensing threshold in the case that W/L is large or small. We apply these analytical results to enhancing a practical WLAN by proposing a robust design method against sensing threshold variation for WLANs.

The rest of this paper is organized as follows. We describe the CSMA/CA network environment under consideration in Section II and propose a CSMA/CA analysis model that captures carrier-sensing errors based on a Markov chain. In

Manuscript received December 12, 2008; revised April 25, 2009 and July 29, 2009. First published November 17, 2009; current version published March 19, 2010. This work was supported by the Ministry of Knowledge Economy, Korea, under the Information Technology Research Center support program supervised by the Institute of Information Technology Advancement under Grant IITA-2009-C1090-0902-0037 and the IT R&D program of the Ministry of Knowledge Economy/Korea Evaluation Institute of Industrial Technology under Grant 2008-F-004-02, 5G mobile communication systems based on beam division multiple access and relays with group cooperation. The review of this paper was coordinated by Dr. P. Lin.

The authors are with the Department of Electrical Engineering, Korea Advanced Institute of Science and Technology, Daejeon 305-701, Korea (e-mail: jw9607@gmail.com; dksung@ee.kaist.ac.kr; ysung@ee.kaist.ac.kr).

Color versions of one or more of the figures in this paper are available online at http://ieeexplore.ieee.org.

Digital Object Identifier 10.1109/TVT.2009.2036927

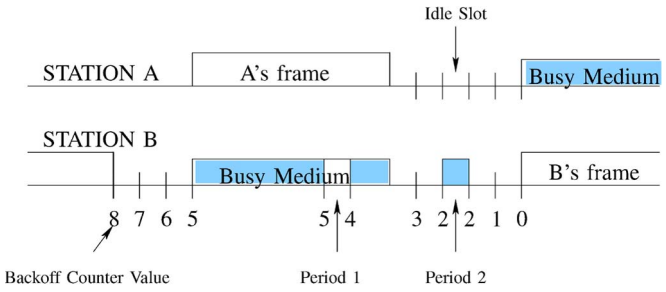

Fig. 1. Operation of the CSMA/CA basic-access protocol.

Section III, we analyze the normalized throughput and mean access delay of the CSMA/CA network in the presence of carrier-sensing errors. The sensitivity of the throughput and delay with respect to the sensing threshold is investigated in Section IV. Analytical and simulation results are presented in Section V. Finally, conclusions follow in Section VI.

II. System Model

A. Operation of CSMA/CA Stations under the Presence of Sensing Errors

We consider a network consisting of n transmitter–receiver pairs operating under the CSMA/CA protocol. To facilitate the analysis, we assume that the system is slotted and synchronized among stations. The backoff stage value corresponds to the current number of retransmissions. We assume that the transmitters have only one backoff stage and that the CW size of the backoff stage is W, and the CSMA/CA stations are in saturated mode, i.e., they always have frames to transmit.[1] In the slotted CSMA/CA, each transmitter senses the channel at the beginning of each slot. If the input signal level of the channel sensor is larger than a predetermined threshold, the CSMA/CA station determines that the channel is busy. Otherwise, it considers the channel to be idle. Here, the sensing is not perfect, and there is a sensing error because of channel impairments such as noise or distortion during the transmission. Typically, there are two types of sensing errors: false alarm and miss detection. A *false-alarm error* is defined as an error that occurs when the sensor determines that the channel is busy when the channel is actually idle. On the other hand, a *miss-detection error* is defined as an error that occurs when the sensor determines that the channel is idle, provided that the channel is actually busy. The false-alarm probability and the miss-detection probability, which are denoted by p_f and p_m, respectively, are generally dependent on the input signal power, noise power, sensing threshold value, and sensor type.

Fig. 1 illustrates the operation of the slotted CSMA/CA for an example of a two-user system. Before a station initiates the transmission of a frame, it senses the channel to determine the availability of the channel. If the channel is sensed to be idle for a backoff unit slot σ, the value of the backoff counter decreases, as in Fig. 1. Otherwise, the station continues to sense the channel until the channel is sensed to be idle for an interval of σ. In Fig. 1, station B experiences both miss-detection and false-alarm errors. For period 1, station B decreases the value of its backoff counter from five to four since station B miss detects the transmission of station A. For period 2, on the other hand, station B freezes its backoff counter since station B has a false-alarm error.

The operation of CSMA/CA nodes is widely modeled using a Markov chain, with states being defined as the values of the backoff counter. We propose a new Markov chain model for the CSMA/CA in the presence of carrier sensing errors at the physical layer. To capture the sensing errors, transitions capturing the sensing-error events are introduced, and the corresponding transition probabilities are assigned from the physical-layer parameters. Fig. 2 shows the proposed model for the operation of each CSMA/CA node capturing the false alarm and miss detection at the sensing stage, where a state transition occurs in every slot. The chain is divided into the right and left sides around state S_0. State S_i in the right part represents that the CSMA/CA station has a backoff counter value of i without transmitting a frame. State S_i in the left part corresponds to the case that the CSMA/CA station is transmitting the $(-i+1)$th slot of a frame with a backoff counter value of zero.

In the states on the right side of the chain, there are two conditions under which the node decreases its backoff counter value; the node decreases its current backoff counter value by one: 1) when the carrier sensor of the node determines that the channel is idle (with a probability of $1-p_f$) when it is actually idle (with a probability of $1-\alpha$, where α is the channel activity factor) or 2) when the carrier sensor of the node declares that the channel is idle (with a probability of p_m) when it is actually busy (with a probability of α). Hence, the transition probability from state S_i to state S_{i-1} is given by $\alpha p_m + (1-\alpha)(1-p_f)$ in the right side of the chain. In addition, looping from state S_i to state S_i is also possible when the carrier sensor declares the presence of a signal in the channel, and the transition probability for this event is given by $(1-\alpha)p_f + \alpha(1-p_m)$. On the left side of the chain, on the other hand, the CSMA/CA node is in the process of transmitting a frame with a length of L slots. When the backoff counter value of the node reaches zero (state S_0), the node starts to transmit a frame. Whether the transmission of each slot of the frame is successful or not, the node continues transmitting the frame, and the state of the node moves to the left until it finishes the transmission of the frame. If the frame transmission is not collided by the transmission of other nodes during the whole frame transmission duration, the frame is successfully transmitted. If at least one of the L slots of the frame is collided, on the other hand, we consider that the frame is collided and that the transmission is not successful. The collision probability is derived in Section II-B. Whether the transmission is successful or collided, the node randomly selects a new value for the backoff counter from $[0, W-1]$ after the transmission. Thus, the state transition for the chain is given in Fig. 2.

The stationary probability distribution is unique since the proposed Markov chain in Fig. 2 is ergodic. From the

[1]Multiple backoff stage cases can be obtained with some modification. In that case, however, the effect of false-alarm and miss-detection errors on the MAC performance is similar.

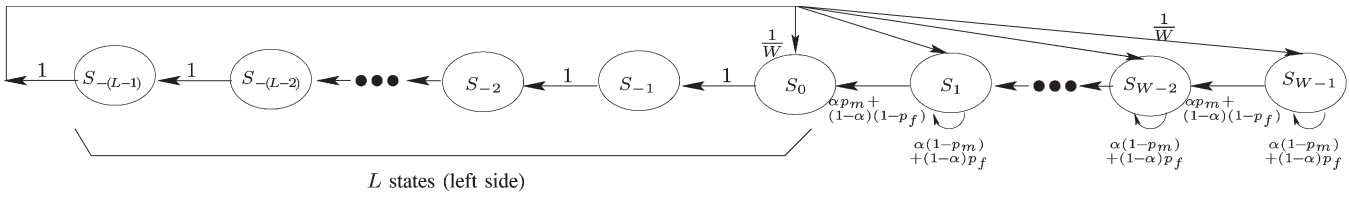

Fig. 2. Markov chain model for a CSMA/CA node with sensing errors ($0 \le p_f, p_m \le 1$).

aforementioned transition probabilities, we obtain the relation between the stationary probabilities as

$$\begin{aligned} P\{S_{i-1}|S_i\} &= \alpha p_m + (1-\alpha)(1-p_f), \qquad i \in [1, W-1] \\ P\{S_i|S_i\} &= \alpha(1-p_m) + (1-\alpha)p_f, \qquad i \in [1, W-1] \\ P\left\{S_{(i-1)}|S_i\right\} &= 1, \qquad i \in [-(L-2), 0] \\ P\left\{S_i|S_{-(L-1)}\right\} &= 1/W, \qquad i \in [0, W-1] \end{aligned}$$

where W denotes the CW size. The term b_i denotes the stationary probability of state S_i. From the aforementioned transition probabilities, we obtain the relationship between stationary probabilities given by

$$\begin{aligned} b_i &= b_0, \qquad i \in [-(L-1), -1] \\ b_i &= \frac{b_0}{\alpha p_m + (1-\alpha)(1-p_f)} \frac{W-i}{W}, \qquad i \in [1, W-1] \end{aligned} \tag{1}$$

and the normalization condition for the stationary distribution is given by

$$1 = b_0 \left\{ L + \frac{1}{\alpha p_m + (1-\alpha)(1-p_f)} \frac{W-1}{2} \right\}. \tag{2}$$

From (1) and (2), we obtain the stationary probability b_0 for state S_0 as a function of p_f, p_m, W, L, and α, which is given by

$$b_0(p_f, p_m, W, L, \alpha) = \frac{2\{\alpha p_m + (1-\alpha)(1-p_f)\}}{2L\{\alpha p_m + (1-\alpha)(1-p_f)\} + (W-1)}. \tag{3}$$

The stationary probabilities for other states are obtained by using (1) based on the b_0 in (3).

B. Collision Probability p_c and Channel Activity Factor α

First, consider the operation of a CSMA/CA network with two pairs of stations, as shown in Fig. 3, under the presence of carrier-sensing errors for illustration. Stations A and B transmit data to stations C and D, respectively. The transmission of data from one transmitter to its corresponding receiver ($A \to C$ or $B \to D$) is successful if no other transmission occurs during the transmission (see periods 1 and 3). If the two transmitters A and B simultaneously start to transmit their data frames, a collision occurs (period 2). This event happens even in the perfect sensing CSMA/CA network, as well as in the imperfect sensing CSMA/CA network. However, either a transmission attempt from transmitter A to receiver C occurs in the middle of the transmission of transmitter B to receiver D (period 4) or the opposite case (period 5) occurs only in the network with imperfect sensing. Hence, these additional collisions need to be considered in modeling the operation of CSMA/CA under the presence of carrier-sensing errors.

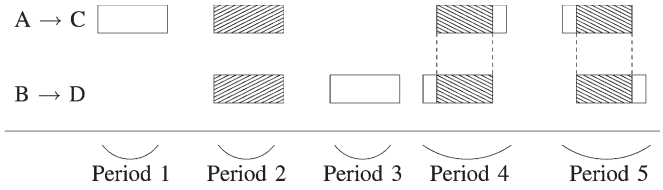

Fig. 3. Data transmission flow time diagram of two pairs of stations in a CSMA/CA network with sensing errors.

In a more general n-transmitter case, the transmission of one station is collided in the middle if some other transmitter in the network is in state S_1 and miss-detects the channel (for example, station B during period 5 in Fig. 3). Let p_{c_l} denote the probability that a transmitted frame of one station is collided from the lth slot due to the transmission of some other station in the network. We assume that p_{c_l} is the same, irrespective of the value of l ($2 \le l \le L$), except for the case of $l = 1$, i.e., $p_{c_2} = p_{c_3} = \cdots = p_{c_L} =: p_c$. Then, p_c is given by

$$\begin{aligned} p_c &= 1 - \left(1 - \frac{b_1}{\sum_{i=1}^{W-1} b_i} \times p_m\right)^{n-1} \\ &= 1 - \left(1 - \frac{2p_m}{W}\right)^{n-1} \end{aligned} \tag{4}$$

where n is the total number of transmitters in the network. Note that $(b_1 / \sum_{i=1}^{W-1} b_i) \times p_m$ is the probability that another transmitter (e.g., station B) among the $n-1$ transmitters other than the station having the ongoing transmission starts a transmission from the backoff stage (conditioned that there is already a transmission going on). The condition that one transmitter is transmitting without collision up to the $(L-1)$th slot of the frame implies that all other stations (including station B) are in the backoff stage up to transmission end time. $b_1 \times p_m$ explains the probability of the further event that the backoff counter value of station B is one and station B miss-detects the channel.

Since α is the probability that the channel is busy from the viewpoint of a particular station, α is the probability that at least one of the other stations is in one of the states in the left part of the Markov chain and is given by

$$\alpha = 1 - \left(\sum_{i=1}^{W-1} b_i\right)^{n-1} \tag{5}$$

where the term $(\sum_{i=1}^{W-1} b_i)^{n-1}$ is the probability that all $n-1$ other transmitters are in the backoff stage, i.e., the right side of the chain in Fig. 2.

III. Analysis of Carrier-Sense Multiple Access/Collision Avoidance in the Presence of Carrier-Sensing Errors

A. Normalized Throughput S and Mean Access Delay D

Our approach to calculate the overall system throughput is based on the symmetry among the CSMA/CA nodes. In other words, one particular node is not favored over other nodes. Hence, we first calculate the per-node throughput of an arbitrary node considering the operation of all the other nodes, and the overall system throughput is given by the product of the number of nodes and the per-node throughput. Our approach is also based on a slot-by-slot approach [17], [18]. That is, for each slot, we calculate the probability that the slot is used for a successful transmission, a collision, or an idle period. We denote P_{bo} as the probability that a station has a positive backoff counter value $(b_i, 1 \le i \le W-1)$. The term τ denotes the probability that a station initiates a transmission conditioned on the fact that the station has a positive backoff counter value and that the channel is not occupied. Then, P_{bo} and τ are given by

$$P_{bo} = \sum_{i=1}^{W-1} b_i \tag{6}$$

$$\tau = \frac{b_1}{\sum_{i=1}^{W-1} b_i}(1-p_f) \tag{7}$$

where p_f is the false-alarm probability. Under the condition, a station initiates a transmission if and only if the station is in state S_1 and does not make a false-alarm error, which explains (7).

The successful transmission, collision, and idle probabilities for the given station, which are denoted by P_S, P_C, and P_I, respectively, are obtained as functions of P_{bo}, τ, p_c, and L using the stationary distribution and are given by

$$P_I = P_{bo}^n (1-\tau)^n \tag{8}$$

$$P_S = n \times P_{bo}^n \tau (1-\tau)^{n-1} \times (1-p_c)^{L-1} L \tag{9}$$

$$P_C = 1 - P_S - P_I. \tag{10}$$

Here, P_{bo}^n represents the probability that the channel is idle at the beginning of the slot, and (8) is obvious. Equation (9) is explained as follows. $P_{bo}^n \tau (1-\tau)^{n-1}$ is the probability that the channel is idle at the beginning of the slot, and one, and only one, user initiates the transmission of a frame. However, the first slot of the frame would not be regarded as a successfully transmitted slot unless the following $L-1$ slots are also successfully transmitted. Here, we assume that the collision probability at each slot is equal to $(1-p_c)$ during $L-1$ slots. Once the event of a successful transmission of a frame occurs, the total L slots are consumed. Factor n represents the fact that the successful transmission of a frame can be done by any of the n transmitters in the network. Thus, the normalized throughput S of CSMA/CA is given by

$$S = \frac{\sigma P_S}{\sigma(P_I + P_S + P_C)} \tag{11}$$

where σ is the slot length. From (10) and (11), S is given by

$$S = n P_{bo}^n \tau (1-\tau)^{n-1} (1-p_c)^{L-1} \times L. \tag{12}$$

Substituting (4), (6) and (7) into (12) yields

$$\begin{aligned} S = n & \left[\frac{1}{\left\{1-(1-Lb_0)^{n-1}\right\} p_m + \left(1-Lb_0^{n-1}\right)(1-p_f)} \frac{W-1}{2} \right]^n \\ & \times \left[\frac{2(1-p_f)}{W} \right] \left[1 - \frac{2(1-p_f)}{W} \right]^{n-1} \\ & \times \left[\left(1 - \frac{2p_m}{W} \right)^{n-1} \right]^{L-1} \times L \end{aligned} \tag{13}$$

where b_0 is obtained from the solution of (3) and is a function of p_m, p_f, W, and L. Note that S is a function of various physical/MAC-layer parameters such as p_m, p_f, W, L, and n.

The delay can easily be obtained by Little's law. Let D be the average access delay defined as the time elapsing between the instant of time that the frame is put into service—i.e., it becomes head of line (HOL)—and the instant of time that the frame is successfully delivered. D is given, using Little's law, by [6]

$$D = \frac{E[n]}{S/E[P]} \tag{14}$$

where P is the payload length (i.e., the frame size in our case), the numerator $E[n]$ represents the average number of competing stations that will successfully deliver their HOL frames, and the denominator $S/E[P]$ represents the frame-delivery rate (i.e., the throughput measured in frames per second). Here, $E[n]$ is equal to the number of CSMA/CA transmitters. The unit of $E[P]$ is a CSMA/CA backoff unit slot.

IV. Sensitivity Analysis: Impact of Sensing Threshold

A. ROCs

For carrier sensing at CSMA/CA nodes, either a matched filter or an energy detector can be used. The matched-filter detector requires knowledge of the signal signature, whereas the energy detector does not. In this section, we consider the commonly used energy detector and matched filter and analyze the sensitivity of the throughput and delay with respect to the sensing threshold.

Assuming that both signal and noise are modeled as white Gaussian[2] processes [19], [20], the sensing problem is given by the following hypotheses test:

$$\begin{cases} H_0 : Y_i \sim \mathcal{N}\left(0, \sigma_0^2\right), & i = 1, \ldots, K \\ H_1 : Y_i \sim \mathcal{N}\left(0, \sigma_0^2 + \sigma_1^2\right), & i = 1, \ldots, K \end{cases} \tag{15}$$

where $\{Y_i\}$ are the observation samples, K is the observation period in slots, and σ_0^2 and σ_1^2 are the noise power and the

[2]For a different signal model, we only need to recalculate p_m and p_f, and all other analyses are still valid with the modification of p_m and p_f.

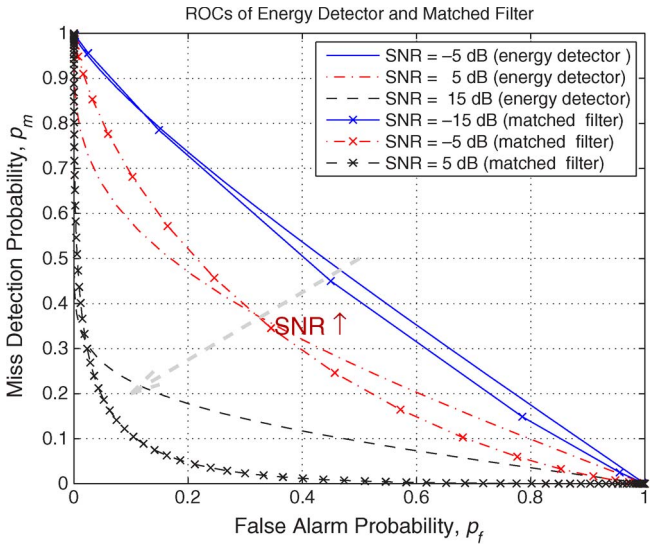

Fig. 4. ROCs of the energy detector and the matched-filter detector ($K = 1$).

signal sample power, respectively.[3] Since the CSMA/CA transmitter senses the channel once in each slot, the value of K in our system is assumed to be one in our system. Under the Neyman–Pearson criterion, the optimal detector is given by

$$\sum_{i=1}^{K} Y_i^2 \underset{<H_0}{\overset{\geq H_1}{}} \eta \tag{16}$$

where η is the sensing threshold. Then, the false-alarm probability p_f and the miss-detection probability p_m for the energy detector are given, respectively, by [21]

$$\begin{aligned} p_f &= \epsilon(\eta) = 1 - \Gamma\left(\frac{K}{2}, \frac{\eta}{2\sigma_0^2}\right) \\ p_m &= \delta(\eta) = \Gamma\left(\frac{K}{2}, \frac{\eta}{2\left(\sigma_0^2 + \sigma_1^2\right)}\right) \end{aligned} \tag{17}$$

where $\Gamma(m, a) = (1/\Gamma(m)) \int_0^a t^{m-1} e^{-t} dt$ is the incomplete gamma function. That is, p_f corresponds to the probability of detecting H_1 when the true hypothesis is H_0, while p_m corresponds to the probability of detecting H_0 when the true hypothesis is H_1.

The operating characteristics of a detector is typically described by the receiver operating characteristic (ROC) curve that shows the miss-detection probability p_m as a function of the false-alarm probability p_f. Fig. 4 shows the ROC of the energy detector and matched-filter detector for several sets of SNR values. The lines with no marks indicate the ROC of the energy detector, whereas the lines with marks indicate that of the matched filter. Here, we set $\sigma_0^2 = 0$ dB in the energy detector. An increase in the sensing threshold for given signal and noise power values moves the operating point toward the upper direction along one of the curves in the figure.

In the matched-filter case, the false-alarm probability p_f^{mf} and the miss-detection probability p_m^{mf} for the optimal Neyman–Pearson detector are given by [21]

$$\begin{aligned} p_f^{mf} &= \epsilon^{mf}(\eta) = Q\left(\frac{\eta}{\sqrt{K}\sigma_0}\right) \\ p_m^{mf} &= \delta^{mf}(\eta) = Q\left(\frac{KE_S - \eta}{\sqrt{K}\sigma_0}\right) \end{aligned} \tag{18}$$

where $Q(x) = \int_x^\infty (1/\sqrt{2\pi}) e^{-t^2/2} dt$, E_s $(= \sigma_1^2)$ is the sample energy, and the overall SNR is given by KE_s/σ_0^2, where K is the number of observation samples.

The ROC of the matched filter for several values of SNR is shown as the lines with marks in Fig. 4. Note that, at the very high SNR regime in Fig. 4, both p_m and p_f can maintain low values, even if the sensing threshold changes much. This is not the case for a low SNR.

B. Sensitivity of Throughput $dS/d\eta$ and Delay $dD/d\eta$

The sensitivity is a measure of the degree of variation of its performance from the nominal value due to the change in the elements in the system. The throughput sensitivity is derived as the derivative of the normalized throughput S with respect to the sensing threshold η. Since S is a function of p_m and p_f, the sensitivity of the throughput $dS/d\eta$ can be expressed as

$$\left|\frac{dS}{d\eta}\right| = \left|\frac{\partial S}{\partial p_f}\frac{dp_f}{d\eta} + \frac{\partial S}{\partial p_m}\frac{dp_m}{d\eta}\right|. \tag{19}$$

Note that the overall sensitivity consists of two terms: the detector characteristics ($dp_f/d\eta$ and $dp_m/d\eta$) and the throughput characteristics ($\partial S/\partial p_f$ and $\partial S/\partial p_m$). This separation makes it easy to consider other types of carrier sensors since a different carrier sensor changes only the detector characteristics. For the energy detector, the detector characteristics $dp_f/d\eta$ and $dp_m/d\eta$ are obtained from (17) and are given by

$$\frac{dp_f}{d\eta} = -\frac{1}{\Gamma\left(\frac{K}{2}\right)} \cdot e^{-\frac{\eta}{2\sigma_0^2}} \cdot \frac{1}{2\sigma_0^2} \cdot \frac{\eta}{2\sigma_0^2}^{\left(\frac{K}{2}-1\right)} \tag{20}$$

$$\frac{dp_m}{d\eta} = \frac{1}{\Gamma\left(\frac{K}{2}\right)} \cdot e^{-\frac{\eta}{2\left(\sigma_0^2+\sigma_1^2\right)}} \cdot \frac{1}{2\left(\sigma_0^2+\sigma_1^2\right)} \cdot \frac{\eta}{2\left(\sigma_0^2+\sigma_1^2\right)}^{\left(\frac{K}{2}-1\right)}. \tag{21}$$

The detector-independent throughput characteristics $\partial S/\partial p_f$ and $\partial S/\partial p_m$ can numerically be obtained by differentiating S with respect to p_f and p_m, respectively, using the obtained throughput S in (13) as a function of p_f and p_m. Substituting (20) and (21) into (19), we have

$$\begin{aligned} \left|\frac{dS}{d\eta}\right| = \Bigg| & -\frac{1}{\Gamma\left(\frac{K}{2}\right)} \cdot e^{-\frac{\eta}{2\sigma_0^2}} \cdot \frac{1}{2\sigma_0^2} \cdot \frac{\eta}{2\sigma_0^2}^{\left(\frac{K}{2}-1\right)} \\ & \cdot \left(\frac{\partial S}{\partial p_f}\right)_{p_f=\epsilon(\eta), p_m=\delta(\eta)} + \frac{1}{\Gamma\left(\frac{K}{2}\right)} \\ & \cdot e^{-\frac{\eta}{2\left(\sigma_0^2+\sigma_1^2\right)}} \cdot \frac{1}{2\left(\sigma_0^2+\sigma_1^2\right)} \cdot \frac{\eta}{2\left(\sigma_0^2+\sigma_1^2\right)}^{\left(\frac{K}{2}-1\right)} \\ & \cdot \left(\frac{\partial S}{\partial p_m}\right)_{p_f=\epsilon(\eta), p_m=\delta(\eta)} \Bigg|. \end{aligned} \tag{22}$$

[3] $\mathcal{N}(0, \sigma^2)$ denotes the zero-mean Gaussian distribution with variance σ^2.

TABLE I
CONSIDERED CSMA/CA AND WLAN PARAMETER VALUES

Parameter	Value	Description
L	[1,47]slots	Length of frame
W	[1, 300]	Contention window (CW) size
$ACK_{wl,11b}$	14 bytes	ACK size
$MACheader_{wl,11b}$	28 bytes	MAC header size
$\sigma^2_{0\,wl,11b}$	0 dB	Noise power
$\sigma^2_{1\,wl,11b}$	15 dB	Transmit power
$R_{wl,11b}$	11 Mbps	Transmission rate
$tSIFS_{wl,11b}$	10 usec	Short interframe space
$tDIFS_{wl,11b}$	50 usec	Distributed interframe space
$tSlot_{wl,11b}$	20 usec	Unit backoff slot length
$tPHYpreamble_{wl,11b}$	144 usec	PHY preamble length
$tPLCPheader_{wl,11b}$	48 usec	PLCP header length
$L_{s,wl}$	22∼47 slots (440∼940μs)	Length of WLAN successful transmission
$L_{c,wl}$	22∼47 slots (440∼940 μs)	Length of WLAN collided transmission
$L_{c,wl}$	22∼47 slots (440∼940μs)	Length of WLAN collided transmission

The sensitivity of delay $dD/d\eta$ can be expressed as

$$\left|\frac{dD}{d\eta}\right| = \left|\frac{\partial D}{\partial p_f}\frac{dp_f}{d\eta} + \frac{\partial D}{\partial p_m}\frac{dp_m}{d\eta}\right|. \tag{23}$$

Substituting (14) into (24), we obtain

$$\left|\frac{dD}{d\eta}\right| = \frac{E[n]}{\left|\frac{dS}{d\eta}\right| \Big/ E[P]}. \tag{24}$$

In the matched-filter case, the detector characteristics $dp_f^{mf}/d\eta$ and $dp_m^{mf}/d\eta$ are obtained from (18), and thus, the corresponding sensitivity can be obtained by substituting these detector characteristics into (22) and (24).

V. NUMERICAL RESULTS

In this section, we investigate the throughput and the delay as functions of the physical-layer sensing parameters p_f and p_m, as well as other CSMA/CA parameters, using both analysis and simulation. Our considered network is a WLAN consisting of multiple transmitter–receiver pairs under false-alarm and miss-detection errors during transmissions due to channel errors or noise. The CSMA/CA parameter setting in our analysis and simulation is shown in the upper part of Table I. The WLAN parameter setting for the WLAN example in Sections V-B and C is shown in the lower part of Table I following [3]. The analytical results are obtained based on the expressions in Section III. The simulation is performed based on the CSMA/CA protocol described in Section II. Each metric is obtained by averaging at least 1000 transmission trials per station.

A. Normalized Throughput and Mean Access Delay

Fig. 5 shows the normalized throughput S and the mean access delay D for the value of p_f from 0 to 1 when p_m is fixed to 0.1. While the CW size W is fixed to 64, the number of users and the frame length L are varied. The solid lines represent the analytical results based on our model, whereas the

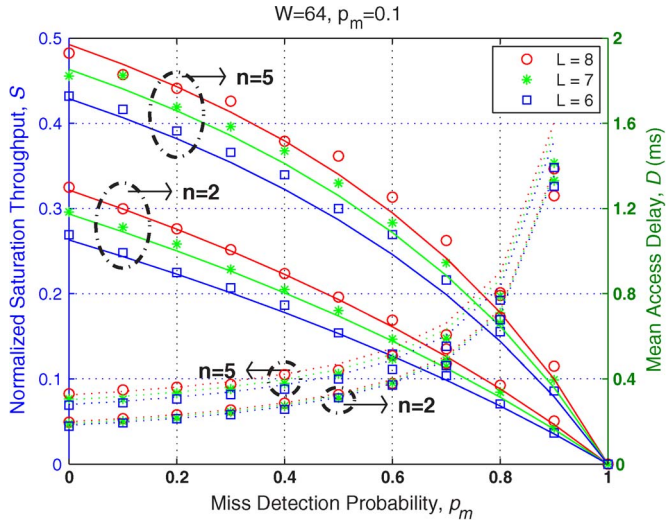

Fig. 5. Normalized throughput S and mean access delay D to vary the false-alarm probability with a fixed miss-detection probability ($0 \le p_f \le 1$, $p_m = 0.1$). (Solid line) Throughput analysis. (Dotted line) Delay analysis. (Mark) Simulation.

simulation results are shown with marks. Each line corresponds to the throughput performance with one fixed L value. It is seen that the simulation results match our analysis well. There are several observations regarding the performance of CSMA/CA as a function of p_f. First, the throughput decreases and the delay increases as the false-alarm probability increases. This is because CSMA/CA stations become more conservative in accessing the channel. In other words, transmitters lose the chance of successful transmissions due to a high sensing threshold. Second, the normalized throughput increases as the frame length L increases. This is because a longer frame occupies more slots when the transmission is successful in this parameter setting. Third, note that the S for $n = 5$ is higher than that for $n = 2$. This implies that the channel is not yet efficiently used when $n = 2$ in the case of $W = 64$. (Of course, all these behaviors depend on L, W, and n.)

Fig. 6 shows the normalized throughput and the mean access delay as a function of p_m ($0 \le p_m \le 1$) with p_f fixed to 0.1. While W is set to 32, the number of users and the frame length are varied. Each line corresponds to the delay performance with one fixed L value. It is observed that the simulation results match our analysis well in this case as well. The behavior of the throughput as a function of p_m depends on W/L. As L is larger, the throughput more steeply decreases since collisions in the middle of a transmission happen frequently because of the large packet size, compared with W.

Fig. 7 shows the behavior of the throughput as a function of p_f and p_m for various sets of CSMA/CA parameters (L and W) obtained from our analysis. Lines without marks and with marks in each subfigure in Fig. 7 represent the throughput corresponding to the values in the ROC curve of an energy detector and a matched filter, respectively. In Fig. 7(a), when the value of the sensing threshold is extremely low, i.e., $\eta = -\infty$, false-alarm and miss-detection errors will occur with probabilities of 1 and 0, respectively. In this case, carrier sensors of CSMA/CA stations always determine that the channel is busy, irrespective of the actual channel status since the false-alarm probability is

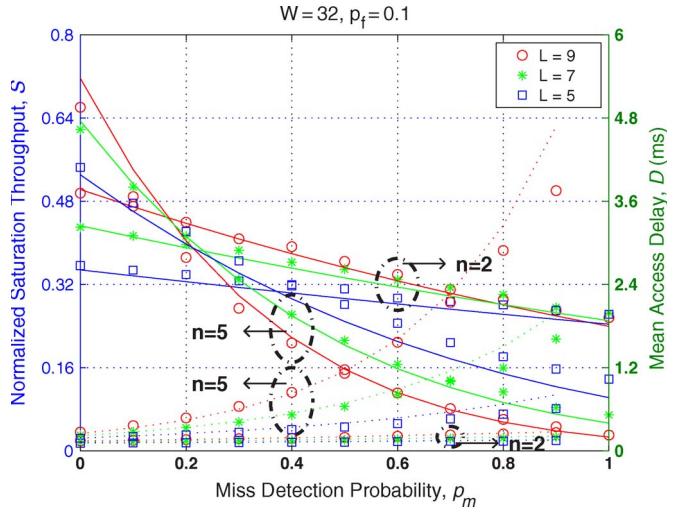

Fig. 6. Normalized throughput S and mean access delay D to vary the miss-detection probability with a fixed false-alarm probability ($0 \leq p_m \leq 1$, $p_f = 0.1$). (Solid line) Throughput analysis. (Dotted line) Delay analysis. (Mark) Simulation.

equal to 1. Eventually, the CSMA/CA stations, in this case, do not transmit their frames at any time. Hence, the operating point of the carrier sensor in this setting ($\eta = -\infty$) is located in the lower rightmost point, i.e., $(p_f, p_m, S) = (1, 0, 0)$. As the sensing threshold value increases, the operating point of the carrier sensor moves toward the upper left direction, following the line whose expression is (17) in the energy-detector case. When the value of the sensing threshold becomes extremely high, i.e., $\eta = \infty$, false-alarm and miss-detection errors will occur with probabilities of 0 and 1, respectively. Hence, the operating point of the carrier sensor in this setting is located in the upper leftmost point, i.e., $(p_f, p_m, S) = (0, 1, z)$, where z is greater than or equal to 0. This tendency is similar to that in the matched-filter case, except for that the line on which the operating point moves following (18). From Fig. 7(a)–(c), it is observed that the ratio W/L is a critical parameter to determine the behavior of the throughput as a function of p_f and p_m. When the ratio is large, the throughput is insensitive to p_m, whereas it is sensitive to p_f, as shown in Fig. 7(a). When the ratio is small, on the other hand, the throughput is insensitive to p_f, while it is sensitive to p_m, as shown in Fig. 7(c). This is explained as follows. For a large value of W/L, the additional sojourn time in the backoff counter's decreasing states due to the extension effect caused by p_f is relatively large since W is large compared with L, and the throughput is more dependent on the p_f value. Since L is small, the chance of collision is already small, and the effect of p_m is negligible. The opposite behavior for a small value of the ratio W/L in Fig. 7(c) is similarly explained. Thus, p_f is a dominant factor for a large W/L, whereas p_m is a dominant factor for a small W/L. At intermediate values of the ratio W/L in Fig. 7(b), the throughput is quite flat in both directions of increasing p_f and p_m near (0, 0) and is thus insensitive to both p_f and p_m. These results suggest that the throughput loss by a poorly chosen sensing threshold, which determines p_f and p_m, is tolerable at intermediate values of the ratio W/L. Another thing to note is that the matched-filter detector shows better performance than the energy detector in Fig. 7, since the matched filter knows the transmitted signal shape.

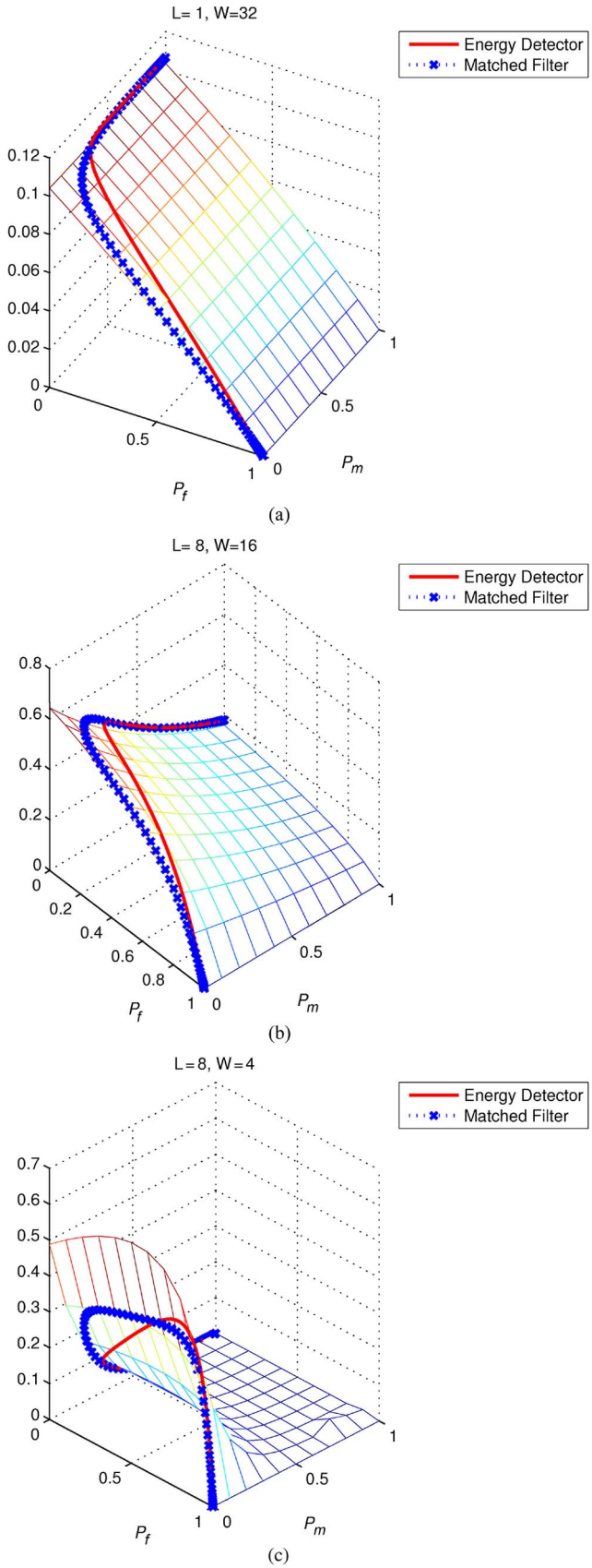

Fig. 7. Normalized throughput S of a CSMA/CA network with a carrier sensor (line without marks: energy detector with SNR = 15 dB, line with marks: matched filter with SNR = 5 dB). (a) $L = 1$, $W = 32$, and $L/W = 0.0313$. (b) $L = 4$, $W = 8$, and $L/W = 0.1250$. (c) $L = 8$, $W = 4$, and $L/W = 2.0000$.

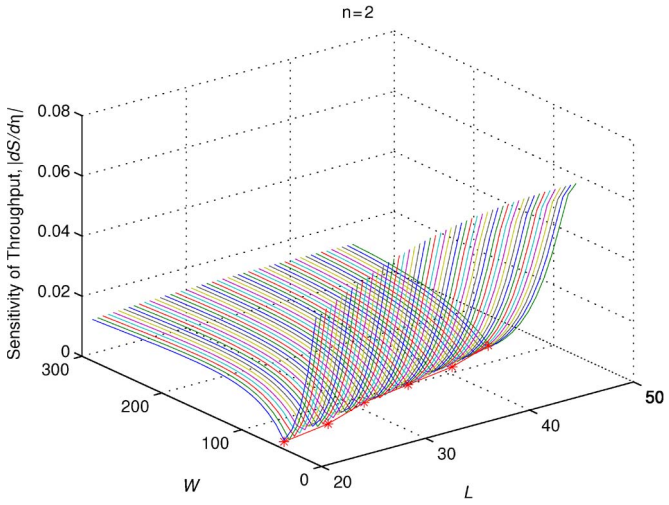

Fig. 8. $dS/d\eta$ for varying W and L when p_f and p_m are set to 0.113 and 0.219, respectively. Energy detector in a WLAN environment ($\sigma_0^2 = 0$ dB and $\sigma_1^2 = 15$ dB).

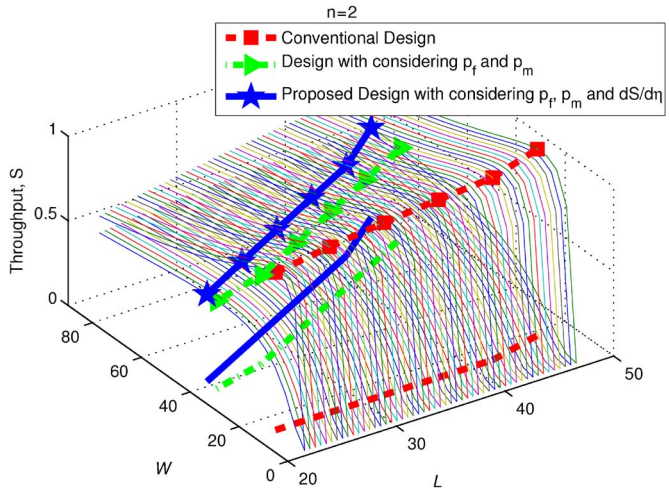

Fig. 9. Normalized throughput S for varying W and L.

B. Sensitivity to the Threshold, $dS/d\eta$, and $dD/d\eta$: WLAN Example

Here, we apply our analysis to WLAN systems. The IEEE 802.11b physical-layer technology is adopted as the physical layer for the CSMA/CA MAC protocol. The IEEE 802.11b physical-layer technology operates in the 2.4-GHz band and is based on direct-sequence spread spectrum. The parameter values relevant to the IEEE 802.11b WLAN CSMA/CA system are shown in the lower part of Table I. In particular, we set the data transmission rate, noise power, and signal power of each station to 11 Mb/s, 0 dB, and 15 dB, respectively. To investigate the relationship among L, W, and sensitivity, we plot the throughput sensitivity with respect to the sensing threshold of an energy detector as a function of L and W in a 3-D plot, as shown in Fig. 8. It is observed that the minimum sensitivity points are well aligned with a line $W = \beta^* L$ for some β^*. When the ratio W/L of the operating CSMA/CA system is away from $W/L = \beta^*$, the throughput is very sensitive with respect to the sensing threshold. Hence, the ratio W/L can be regarded as an important design parameter for CSMA/CA with sensing errors to determine the sensitivity of the system with respect to the carrier sensor design at the physical layer. Thus, care should be taken for the carrier sensor design for extreme values of W/L to not degrade the system throughput by the poor design of the sensing threshold. The minimum sensitivity points in the matched-filter detector can be different from those in the energy detector since the matched filter has a different ROC compared with that of the energy detector.

C. Robust Design Against Sensing Threshold Variation: WLAN Example

Fig. 9 shows the throughput versus L and W values. The 3-D plot with rectangular marks represents the throughput as a function of L and W in 3-D when we assume that no sensing errors exist. In this setting, the throughput is maximized when the CW is in the range of [15, 20] for the L range from 22 to 47 slots. The 3-D plot with triangular marks also shows the throughput for the fixed sensing threshold as a function of L and W for an energy detector. The maximum throughput is obtained at the CW value that is linearly dependent on L. Compared with the no-sensing-error case of the 3-D plot with rectangular marks, the energy detector shows the maximum throughput when the W/L ratio is high, i.e., approximately 3/2.

However, there exists a performance degradation caused by the sensitivity of parameters, i.e., η, from the careless design of carrier sensors, as explained in Section IV-B. We need to obtain the maximum throughput considering this sensitivity to the sensing threshold. If the sensitivity of throughput is high at the maximum throughput point, the throughput can be much degraded with respect to the threshold variation. This degradation can result in smaller throughput than that at the nonmaximum throughput point. Thus, we define a new optimization criterion Z given by

$$Z = S - \lambda |dS/d\eta| \tag{25}$$

where λ is the weighting factor for the sensitivity. By maximizing the new cost Z for a properly chosen λ, we can achieve high throughput with reasonable robustness against the sensing threshold variation. The 3-D plot with star marks in Fig. 9 shows Z when λ is set to 1.2589 (equal to 1 dB) in the energy-detector case. The W/L ratio that maximizes the throughput is approximately 2. This value is increased compared with that for the case when the throughput sensitivity is not considered, as in the 3-D plot with triangular marks in Fig. 9. Hence, it is beneficial to design the CW size W and the frame size L by considering the carrier sensing error and sensitivity to stably and robustly obtain the high throughput.

VI. Conclusion

We have analyzed the performance of the CSMA/CA protocol under carrier-sensing errors. We have obtained the normalized throughput and the mean access delay using a modified Markov chain model that captures both types of sensing errors: false alarm and miss detection. We have further investigated the properties of the throughput and the delay as functions of the false-alarm and miss-detection probabilities. The behavior

of the throughput as a function of the false-alarm and miss-detection probabilities depends on other CSMA/CA parameters such as the CW size W and the frame length L. Simulation results are provided to verify our analysis. The ratio W/L is a key parameter to determine the sensitivity of the throughput with respect to the channel-sensing threshold.

REFERENCES

[1] L. Kleinrock and F. Tobagi, "Packet switching in radio channels: Part I—Carrier sense multiple-access modes and their throughput-delay characteristics," *IEEE Trans. Commun.*, vol. COM-23, no. 2, pp. 1400–1416, Dec. 1975.

[2] H. Takagi and L. Kleinrock, "Throughput analysis for persistent CSMA systems," *IEEE Trans. Commun.*, vol. COM-33, no. 7, pp. 627–638, Jul. 1985.

[3] *Wireless LAN Medium Access Control (MAC) and Physical Layer (PHY) Specifications*, IEEE Std. 802.11 WG, Jun. 1997.

[4] *Part 15.4: Wireless Medium Access Control (MAC) and Physical Layer (PHY) Specifications for Low-Rate Wireless Personal Area Networks (LR-WPANs)*, IEEE Std. 802.15.4, 2003.

[5] G. Bianchi, "Performance analysis of the IEEE 802.11 distributed coordination function," *IEEE J. Sel. Areas Commun.*, vol. 18, no. 3, pp. 535–547, Mar. 2000.

[6] G. Bianchi and I. Tinnirello, "Remarks on IEEE 802.11 DCF performance analysis," *IEEE Commun. Lett.*, vol. 9, no. 8, pp. 765–767, Aug. 2005.

[7] H. Wu, Y. Peng, K. Long, S. Cheng, and J. Ma, "Performance of reliable transport protocol over IEEE 802.11 wireless LANs: Analysis and enhancement," in *Proc. IEEE INFOCOM*, 2002, vol. 2, pp. 599–607.

[8] P. Chatzimisios, A.C. Boucouvalas, and V. Vitsas, "IEEE 802.11 packet delay—A finite retry limit analysis," in *Proc. IEEE Globecom*, 2003, pp. 950–954.

[9] S. Pollin, M. Ergen, S. C. Ergen, B. Bougard, L. Van der Perre, F. Cathoor, I. Moerman, A. Bahai, and P. Varaiya, "Performance analysis of slotted IEEE 802.15.4 medium access layer," Tech. Rep., DAWN Project, Sep. 2005. [Online]. Available: http://www.soe.ucsc.edu/research/ccrg/DAWN/papers/ZigBee_MACvPV.pdf

[10] J. Misic, S. Shafi, and V. B. Misic, "Performance of a beacon enabled IEEE 802.15.4 cluster with downlink and uplink traffic," *IEEE Trans. Parallel Distrib. Syst.*, vol. 17, no. 4, pp. 361–376, Apr. 2006.

[11] T. R. Park, T. H. Kim, J. Y. Choi, S. Choi, and W. H. Kwon, "Throughput and energy consumption analysis of IEEE 802.15.4 slotted CSMA/CA," *Electron. Lett.*, vol. 14, no. 18, pp. 1017–1019, Sep. 2005.

[12] C. Y. Jung, H. Y. Hwang, D. K. Sung, and G. U. Hwang, "Enhanced Markov chains model and throughput analysis of the slotted CSMA/CA of the IEEE 802.15.4 under an unsaturated traffic condition," *IEEE Trans. Veh. Technol.*, vol. 58, no. 1, pp. 473–478, Jan. 2009.

[13] L. Krishnamurthy, J. Zhu, X. Guo, L. L. Yang, and W. S. Conner, "Making radios more like human ears," *Mesh Network Summit*, 2004. [Online]. Available: http://research.microsoft.com/en-us/um/redmond/events/meshsummit/Presentations/DayOne/session1/LakshmanKrishnamurthy.ppt

[14] J. A. Fuemmeler, N. H. Vaidya, and V. V. Veeravalli, "Selecting transmit powers and carrier sense thresholds for CSMA protocols," Univ. Illinois, Urbana-Champaign, IL, Tech. Rep., Sep. 2001.

[15] J. W. Chong, Y. Sung, and D. K. Sung, "Cross-layer performance analysis for CSMA/CA systems: Impact of imperfect sensing," in *Proc. IEEE SPAWC*, Jul. 2008, pp. 96–100.

[16] J. W. Chong, Y. Sung, and D. K. Sung, "Analysis of CSMA/CA systems under carrier sensing error: Throughput, delay and sensitivity," in *Proc. IEEE Globecom*, Dec. 2008, pp. 1–6.

[17] E. Ziouva and T. Antonakopoulos, "CSMA/CA performance under high traffic conditions: Throughput and delay analysis," *Comput. Commun.*, vol. 25, no. 3, pp. 313–321, Feb. 2002.

[18] C. H. Foh and J. W. Tantra, "Comments on IEEE 802.11 saturation throughput analysis with freezing of backoff counters," *IEEE Commun. Lett.*, vol. 9, no. 2, pp. 130–132, Feb. 2005.

[19] J. H. Winters, "Optimum combining in digital mobile radio with cochannel interference," *IEEE Trans. Veh. Technol.*, vol. VT-33, no. 3, pp. 144–155, Aug. 1984.

[20] Y. Chen, Q. Zhao, and A. Swami, "Joint design and separation principle for opportunistic spectrum access in the presence of sensing errors," *IEEE Trans. Inf. Theory*, vol. 54, no. 5, pp. 2053–2071, May 2008.

[21] H. V. Poor, *An Introduction to Signal Detection and Estimation*, 2nd ed. New York: Springer-Verlag, 1994.

Jo Woon Chong received the B.S., M.S., and Ph.D. degrees in electrical engineering from the Korea Advanced Institute of Science and Technology (KAIST), Daejeon, Korea, in 2002, 2004, and 2009, respectively.

Since 2003, he has been a Teaching and Research Assistant with the School of Electrical Engineering and Computer Science, KAIST. His research interests include cognitive radios systems, cross-layer design for communication systems, resource management, multiple access technologies for wireless local area networks and wireless personal area networks, and ultra-wideband communication systems.

Dan Keun Sung (S'80–M'86–SM'00) received the B.S. degree in electronics engineering from Seoul National University, Seoul, Korea, in 1975 and the M.S. and Ph.D. degrees in electrical and computer engineering from the University of Texas at Austin in 1982 and 1986, respectively.

Since 1986, he has been with the faculty of the Korea Advanced Institute of Science and Technology (KAIST), Daejeon, Korea, where he is currently a Professor with the Department of Electrical Engineering. From 1996 to 1999, he was the Director of the Satellite Technology Research Center, KAIST. He was the Division Editor of the *Journal of Communications and Networks*. His research interests include mobile communication systems and networks, with special interest in resource management, wireless local area networks, wireless personal area networks, high-speed networks, next-generation internet-protocol based networks, traffic control in wireless and wireline networks, signaling networks, intelligent networks, performance and reliability of communication systems, and microsatellites.

Dr. Sung is a member of the National Academy of Engineering of Korea. He was the recipient of the 1992 National Order of Merits, the Dongbaek Medal, the 1997 Research Achievement Award, the 1997 MoMuc Paper Award, the 2000 Academic Excellent Award, the 2000 Best Paper Award from the Asia-Pacific Conference on Communications, the 2004 This Month's Scientist Award from the Ministry of Science and Technology and the Korea Science and Engineering Foundation, and the 2005 Paper Award from the Next Generation PC International Conference. He is the Editor of the *IEEE Communication Magazine*.

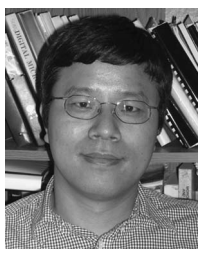

Youngchul Sung (S'92–M'93–SM'09) received the B.S. and M.S. degrees in electronics engineering from Seoul National University, Seoul, Korea, in 1993 and 1995, respectively, and the Ph.D. degree in electrical and computer engineering from Cornell University, Ithaca, NY, in 2005.

He is currently an Assistant Professor with the Department of Electrical Engineering, Korea Advanced Institute of Science and Technology, Daejeon, Korea. From 2005 to 2007, he was a Senior Engineer with the Corporate R&D Center, Qualcomm, Inc., San Diego, CA. His research interests include statistical signal processing, large-deviation theory, graphical models and statistical inference, and signal and information processing for large networks.

Dr. Sung has been a Technical Program Committee member of several conferences, including the IEEE Global Telecommunications Conference (Globecom) in 2009 (where he was also a Session Chair) and 2010, the International Symposium on Conference Modeling, and Optimization in Mobile, Ad Hoc, and Wireless Networks in 2009, the Asia Pacific Signal and Information Processing Association (APSIPA) Annual Summit and Conference in 2009 and 2010, and IEEE Sensor Array and Multichannel Signal Processing Workshop in 2008. He has served as an External Expert Reviewer for the International Conference on Acoustics, Speech, and Signal Processing from 2008 to 2010.